The Asian Monsoons as a Unified System

Ruth Geen[1], F. Hugo Lambert[1]and Geoffrey K. Vallis[1]

[1]College of Engineering, Mathematics and Physical Sciences, University of Exeter, North Park Road, Exeter, Devon EX4 4QF, United Kingdom.

Key Points:

- Idealized model simulations indicate that the Asian monsoon is not just a passive response to insolation, but actively propagates eastward.
- Consistent behavior is observed in the JRA-55 reanalysis and CMAP observations, explaining the regional characteristics of the monsoon.
- This suggests that monsoon change and variability may be understood as change in how a propagating wave interacts with the background state.

Corresponding author: Ruth Geen, `r.geen@exeter.ac.uk`

Abstract

Asian monsoon rainfall impacts one third of the global population and predicting its variability and future change is of clear importance. However, the dynamics of even the climatological monsoon are not fully understood; seemingly unconnected behaviors and abrupt jumps in rainfall location occur in different regions through the year. Three independent subsystems have traditionally been considered: the East Asian, South Asian, and Western North Pacific monsoons. These are generally viewed as passive stationary-wave responses to insolation, but this picture cannot explain the abrupt jumps in rainfall location. Using model simulations, reanalysis and observations, we show that the complex behavior of all three subsystems in fact results from active *propagation* of the summertime 'stationary' wave. A continent-scale cyclone first expands northwestwards and then propagates eastwards via advective and evaporative feedbacks. We propose that the monsoon's response to forcings may be understood by considering how this wave interacts with the background state.

Plain Language Summary

Asian monsoon rainfall impacts one third of the global population and predicting its year-to-year variations and future change is of clear importance. A first step towards this goal is to fully understand the controls on the monsoon in the present climate. Each summer, as the Asian continent warms, the prevailing winds abruptly reverse direction from north-easterly to south-westerly, bringing warm, moist air over the land and causing the onset of the monsoon rains. However, rain does not arrive and end simultaneously across the continent. Instead, seemingly unconnected behaviors and abrupt jumps in rainfall location occur in different regions through the year. Here, we use model simulations with simplified continents, alongside observations, to explore the processes responsible. The monsoon is generally seen as a *passive* response to the warming of the summer hemisphere by insolation, but this cannot explain the abrupt jumps in rainfall location. We show that the complex regional behavior in fact results from the *active* eastward propagation of the summertime circulation. This new picture of the Asian monsoons puts regional rainfall in the context of the larger-scale circulation, and may be useful in guiding how we understand the monsoon's response to global warming and variations in ocean temperature.

1 Introduction

The Asian monsoon rains arrive in multiple stages, developing first over the Bay of Bengal, Indochina Peninsula, and South China Sea in mid-May, and then advancing northwestward over India through June (Wang & LinHo, 2002; Bollasina & Ming, 2013; Parker et al., 2016). Rain later extends abruptly eastward over the Western North Pacific in mid-late July (Wu & Wang, 2001); the mechanism for the onset of this so-called marine monsoon has long remained mysterious (Hsu et al., 2014). These differences in monsoon behavior across the continent (e.g. Fig. 1a) have resulted in the separate study of three distinct components to the Asian monsoon: the East Asian, South Asian and Western North Pacific monsoons (Wang & LinHo, 2002). Interannual variability and patterns of future change in these sub-monsoons are key foci of research, motivated by the significant impacts on global food supply (Gadgil & Gadgil, 2006; Naylor et al., 2007; Cui & Shoemaker, 2018). However, the interactions and basic climatological evolution of these systems are still not well understood (Bollasina & Ming, 2013; Hsu et al., 2014; Parker et al., 2016; Geen et al., 2020). Weak foundations limit our prospects for understanding the monsoons' more complicated aspects and so for predicting their behavior on both seasonal timescales and in future climates.

Observational data show how the monsoons evolve, but the wide range of processes at work make it hard to identify mechanisms in these datasets. Idealized modeling com-

plements the study of observations, allowing continents, orography and physical processes to be added incrementally. Two idealized modeling approaches have commonly been used to study the monsoons: aquaplanets (Earth-like planets with an entirely water-covered surface), to explore controls on zonal-mean tropical rainfall location (Privé & Plumb, 2007) and its seasonality (Bordoni & Schneider, 2008, 2010; Geen et al., 2018, 2019); and steady-state experiments with continents or localized forcing, to explore controls on the seasonal-mean summertime stationary-wave pattern (Matsuno, 1966; Gill, 1980; Rodwell & Hoskins, 2001; Shaw, 2014). However, a unified picture that accounts for both zonal asymmetries and seasonal evolution is missing, leaving a wide gap in understanding between theories that emerge from highly abstracted simulations and results based on observations and comprehensive models.

Here we utilize reanalysis circulation and observational rainfall data and idealized model simulations with simple continents to at last bridge this gap and provide a full description of how the three-dimensional circulation interacts with moisture. Our findings lead us to question the extent to which the Asian monsoons should be considered separately, and to which the summertime circulation pattern can be described as a 'stationary' wave. Section 2 describes the simulations performed and datasets used. In Section 3 we describe the progression of the monsoon across the continent in the observations and simulations. Interactions between the circulation and distribution of temperature and humidity are discussed in Section 4. Section 5 explores the implications of our results in the context of the literature.

2 Methods

2.1 Idealized model simulations

We use the Isca modelling framework (Vallis et al., 2018), which is based on the GFDL spectral dynamical core, and includes a range of parametrisations for simulating the atmospheres of Earth and other planets. The set-up used is similar to the Model of an Idealized Moist Atmosphere (Jucker & Gerber, 2017). The model is configured with the RRTM radiation scheme (Mlawer et al., 1997; Clough et al., 2005) and simple parametrisations of moist physics and convection (Frierson et al., 2006, 2007; O'Gorman & Schneider, 2008). RRTM calculates radiative heating based on the local humidity and temperature every 3600s of model time. As is common in idealized models, clouds are not included in the parametrisations of radiation or moist processes. The insolation includes a seasonal and diurnal cycle, with a solar constant of $1360\mathrm{Wm}^{-2}$, an Earth-like obliquity of 23.429° and a circular orbit. Simulations are run at T42 resolution, with 40 vertical uneven sigma levels and a 720s time-step. Data is interpolated onto a pressure grid at 50-hPa spacing during post-processing. A 360-day calendar is used, so that each model month is 30 days and a year comprises 72 pentads. The model is spun-up for 10 years and then run for a further 30 years. Data from this 30 year period are then used to produce a climatology.

Results from three simulations are presented. In the first, *half-land*, the entire Eastern Hemisphere is prescribed as land, with a slab ocean with heat capacity equivalent to a 2m mixed layer depth, and an albedo of 0.325. An evaporative resistance, α is used to modify evaporation, E, as

$$E = \alpha \rho_a C |\mathbf{v}_a| (q_s - q_a) \tag{1}$$

where ρ_a, $|\mathbf{v}_a|$ and q_a are the density, horizontal wind speed, and specific humidity at the lowest model level respectively. C is the drag coefficient and q_s is the saturation specific humidity at the surface temperature. Over ocean, α is set to 1 and there is no resistance to evaporation; over land $\alpha = 0.7$. Ocean is modelled with a 20m mixed layer depth and an albedo of 0.25, with the high value compensating for the lack of clouds in the model. In the second simulation, *simple-Asia*, land is further confined to the Northern Hemisphere, and an idealized Tibetan Plateau is introduced, with height, z, described

by (Saulière et al., 2012):

$$z = z_0 e^{-\delta_1^2} (1/\delta_2) e^{-0.5(\ln \delta_2)^2} \quad (2)$$

$$\delta_1 = [(x - x_0)\cos(\gamma_1) + (y - y_0)\sin(\gamma_1)]/L_1 \quad (3)$$

$$\delta_2 = [-(x - x_0)\sin(\gamma_2) + (y - y_0)\cos(\gamma_2)]/L_2 \quad (4)$$

where $z_0 = 5700$m, $(x_0, y_0) = (130., 28.)$, $\gamma_1 = -49.5°$, $\gamma_2 = -18°$, and $L_1 = L_2 = 12.5°$. To reduce the effect of Gibbs ripples resulting from spectral truncation of the topography, the smoothing of Lindberg and Broccoli (1996) is applied over both land and ocean. This has the effect of slightly reducing the elevation, but the mountain height is still sufficient to generate a similar impact on the circulation to that seen in reanalysis. The last simulation, *half-land-sn2*, is configured as *half-land*, but with the orbital period doubled, so that the seasonal cycle progresses at half the rate, and mixed layer depths doubled, so that the amplitude of the SST seasonality remains similar. This allows processes paced by dynamics to be distinguished from those paced by insolation.

Key elements lacking from our simulations are clouds and a more complex description of land hydrology. In spite of this, the experiments mimic the behavior seen in observations and reanalysis well (Figs. 1 and 2).

2.2 Reanalysis and observations

The Japanese 55-year Reanalysis (JRA-55; Kobayashi et al., 2015) dataset is used for winds, specific humidity, temperature and geopotential height. For precipitation, the CPC Merged Analysis of Precipitation (CMAP; P. Xie & Arkin, 1997) dataset is used, due to the long record of daily data available. In both cases a climatology is evaluated using years 1979-2016. Repeating our analysis of the precipitation using the GPCP dataset (Huffman et al., 2001) for the years 1997-2015, confirmed the choice of dataset does not influence our results (not shown).

3 Seasonal Progression of Monsoon Rain

Fig. 1a shows Northern Hemisphere monsoon onset timing. The different phases of monsoon onset (Wang & LinHo, 2002) are apparent from the shading, with a band of earlier rain across the Indochina Peninsula and up the coast, a delay before the rains spread northwestward over India, and later onset over the Western North Pacific. The detailed structure shown in Fig. 1a is complex, and might be assumed to be the product of the configuration of the Asian continent and Indian Ocean basins. Fig. 1b shows the onset map for the *half-land* simulation. Despite the lack of meridional asymmetry or orography, we find that this simple configuration in fact reproduces much of the observed onset structure. A band of earlier onset, oriented from south-west to north-east, extends from the centre of the continent up to the eastern coastline. Precipitation expands first northwestward, and later eastward out over the ocean. In the *simple-Asia* simulation (Fig. 1c) these similarities are further amplified. The earliest arrival of precipitation is now in the areas to the south and east of the Plateau, mimicking the behavior observed over the Bay of Bengal and South China respectively.

Maps of climatological-mean precipitation, and zonal wind and pressure anomalies (Fig. 2) help in understanding the patterns in Fig. 1. As the continent warms in spring in the *half-land* simulation, a planetary-scale low-pressure anomaly develops, with an associated cyclonic flow. This flow strengthens as the land-sea energetic contrast intensifies. By pentad 38 tropical precipitation has moved north over the continent, with the southwesterly flow generated near the east coast converging moisture into an intense rainband with a north-eastward extension over the ocean into the subtropics. From pentads 44-56, the region of most intense convection and, coupled to this, the monsoon cyclone itself, travel eastward, displaying a wave-like behavior. The result is later monsoon on-

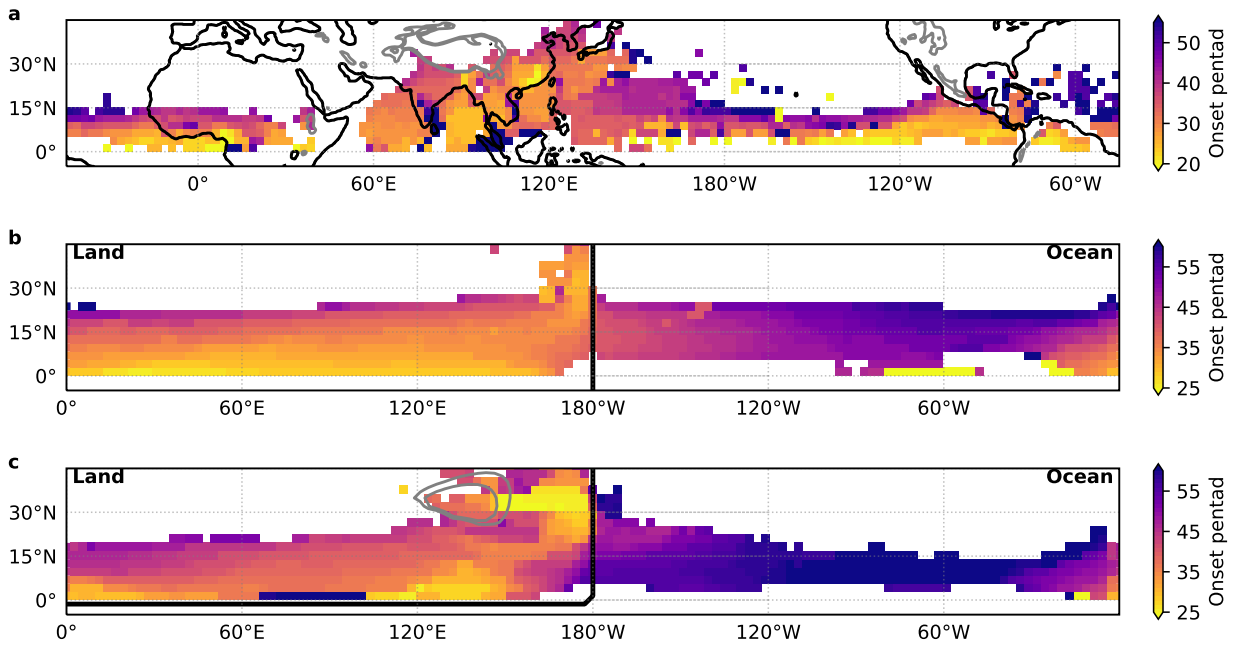

Figure 1. Northern Hemisphere climatological monsoon onset pentad, defined as the pentad at which rainfall exceeds the January mean by at least 5mm/day (Wang & LinHo, 2002), evaluated using (a) CMAP data, (b) data from the half-land simulation, (c) data from the simple-Asia simulation. Black contours show coastlines, and grey contours show 2 and 3km orography contours. Note that in (c) land is confined to the Northern Hemisphere. White indicates areas where the onset criteria is not reached.

set over the ocean to the east. Monsoon onset has been noted to occur rapidly compared to the seasonal evolution of the insolation that drives it (Yin, 1949; S.-P. Xie & Saiki, 1999). To determine whether the wave propagation seen in Fig. 2 is paced by the solar forcing or by dynamics, we compare the cyclone's eastward propagation rate over the ocean in *half-land* with the *half-land-sn2* simulation, in which the year length is doubled so the insolation evolves more slowly. The slowed forcing delays the development of the land-sea contrast, and so the low-pressure anomaly. However, the mature monsoon gyre propagates eastward at a similar rate in both simulations (Fig. S1). This suggests that the summertime 'stationary' waves are not in fact stationary, nor simply governed by the seasonal cycle, but instead self-propagate in part by coupling with convection.

The rightmost column of Fig. 2 shows equivalent maps based on observations and reanalysis. Again, the low pressure centre and cyclonic flow intensify at the start of the summer season, drawing precipitation northward off the Equator, and the cyclonic flow and precipitation later extend eastward. Notable differences to *half-land* are the delay in onset over India following the arrival of precipitation over South-East Asia, and the slower, more limited eastward spread of the monsoon. Data from the *simple-Asia* simulation (middle column) suggest these differences relate to the influence of the Tibetan Plateau on the circulation; mechanisms are explored below.

Overall, the simulations highlight that the spatial and temporal structure of monsoon onset is a consequence of how the large-scale cyclonic flow expands over the continent in summer, with the Tibetan Plateau influencing local characteristics. Timing and intensity differ regionally, but the Asian monsoons are intrinsically connected.

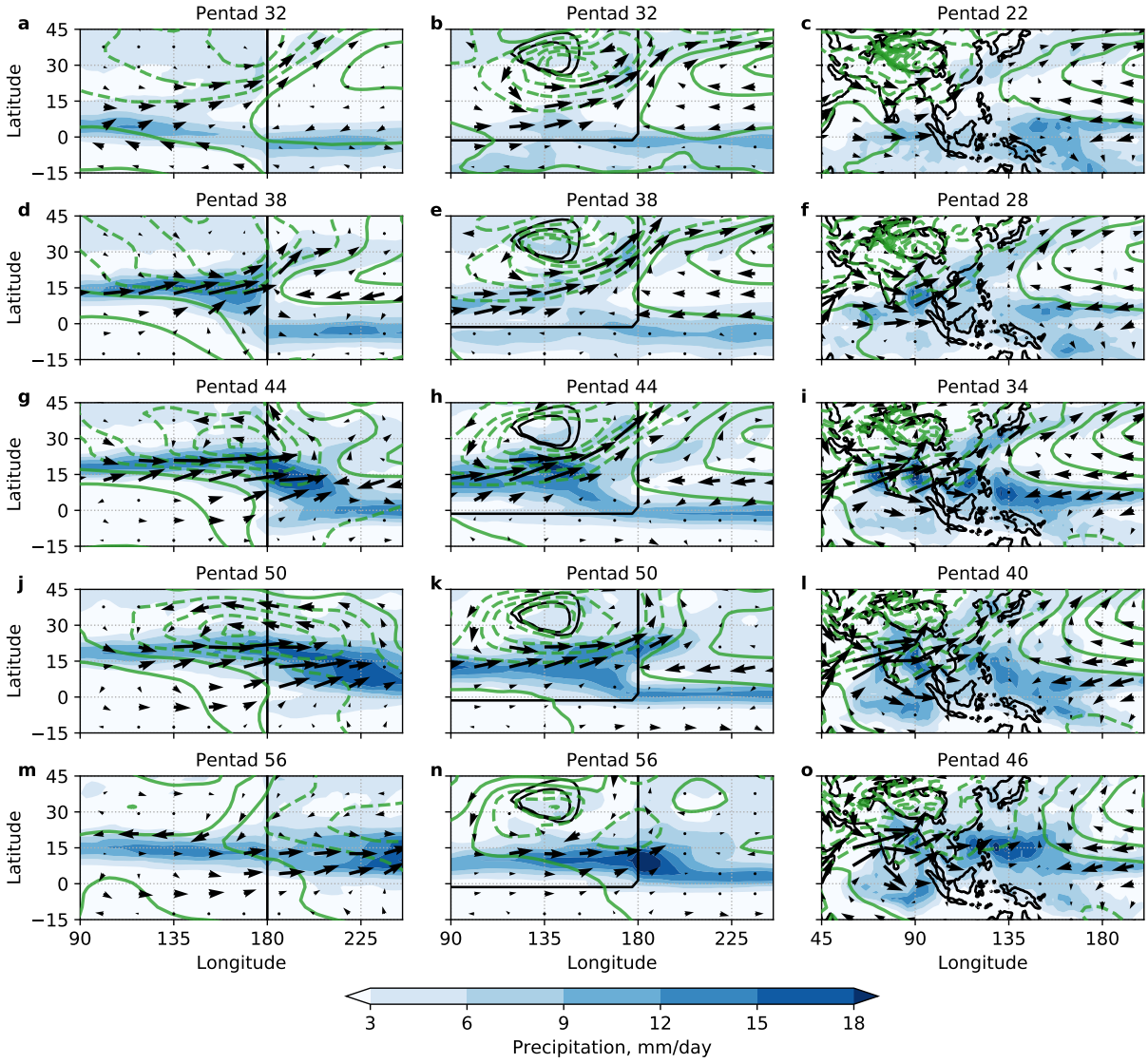

Figure 2. Maps of precipitation (colors), and of 850-hPa wind (arrows) and sea level pressure (grey contours) anomalies relative to the zonal mean. Black contours show the coastlines, and 2 and 3km orography contours. Left column shows data from half-land, centre column shows data from simple-Asia, right column shows CMAP and JRA-55 data. Data are climatological means; the pentads used are indicated by the panel titles.

4 Circulation-Moisture Feedbacks

Monsoon flows involve complex interactions of the tropical overturning circulations with moist processes and the land surface, so building a conceptual understanding of their dynamics is challenging. Moist static energy (MSE), h, describes an air parcel's potential energy and moist enthalpy:

$$h \equiv c_p T + gz + L_v q_v. \tag{5}$$

Here, c_p is the specific heat of air at constant pressure; T is temperature; g the gravitational constant; z geopotential height; L_v is the latent heat of vaporisation of water and q_v is specific humidity. Theory developed in aquaplanets indicates that the subcloud MSE distribution is strongly tied to the location of ascent in the Hadley circulation, if two assumptions can be made. First, the zonal-mean overturning circulation is assumed to conserve angular momentum, with extratropical eddies playing a negligible role. Second, in the tropical atmosphere, convection is assumed to occur rapidly and, on average, maintain a moist adiabatic lapse rate. If these assumptions apply, the divide between the two Hadley cells is colocated with the tropical maximum in subcloud MSE (Privé & Plumb, 2007). When this maximum occurs away from the Equator, the strongest convergence and rainfall lie nearby on its equatorward side. The first assumption has been shown to be particularly relevant to monsoon circulations, which suppress extratropical eddy propagation to low latitudes (Schneider & Bordoni, 2008). The second assumption, Convective Quasi-Equilibrium (CQE) (Betts, 1982; Emanuel, 1995), is observed in the Asian monsoon region (Nie et al., 2010). If these ideas can be extended to Earth's local tropical overturning, then the MSE budget can be used not just to diagnose where convection might occur, but to interpret how feedbacks with the circulation influence the seasonal migration of the ITCZ (Bordoni & Schneider, 2008) and monsoon rain.

Although strictly it is the subcloud MSE that is connected to the distribution of precipitation in the tropics (Privé & Plumb, 2007) because the tropical atmosphere is close to CQE, the column-integrated MSE strongly reflects the low-level distribution (not shown). The vertically-integrated MSE budget has the advantage of indicating how the column is fed MSE by surface heat fluxes:

$$\frac{\partial\{\overline{\mathcal{E}}\}}{\partial t} = \overline{F}_{net} - \left\{\overline{u}\frac{\partial\overline{h}}{\partial x}\right\} - \left\{\overline{v}\frac{\partial\overline{h}}{\partial y}\right\} - \left\{\overline{\omega}\frac{\partial\overline{h}}{\partial p}\right\} - \nabla\cdot\{\overline{h'\mathbf{v}'}\} \tag{6}$$

$$\mathcal{E} \equiv c_v T + gz + L_v q_v \tag{7}$$

$$F_{net} \equiv LH + SH + R_{toa} + R_{surf}. \tag{8}$$

Here, $\mathcal{E}$ is the sum of internal, latent and potential energy and c_v is the specific heat of air at constant volume. u, v, and ω are the zonal, meridional, and vertical wind speeds, and $\mathbf{v}$ is the horizontal wind vector. F_{net} is the net flux of energy from latent, LH, and sensible, SH, heat fluxes, and radiative fluxes at the top of atmosphere, R_{toa}, and surface, R_{surf} (sign convention is that fluxes directed into the atmosphere are positive). Overbars indicate the local climatological pentad mean, and primes deviations from this. Curly brackets indicate column-mass integrals: $\{X\} \equiv \int_0^{p_s} X dp/g$, where p_s is surface pressure. Eq. 7 describes how the internal energy of a column of air is affected by the net diabatic heat fluxes into the column, advection of MSE by the climatological mean flow, and transient eddy fluxes of MSE. The lefthand columns of Figs. 3 and 4 show column integrated MSE (shading) and precipitation (blue contours), confirming that the tropical precipitation tends to lie just equatorward of the peak in column-integrated MSE, even when zonal asymmetries are included. The contribution from eddies was found to be comparatively small in magnitude and is not presented here.

The MSE budget of the *half-land* simulation (Fig. 3) shows how the cyclonic flow over the continent advects warm, humid air and evaporates moisture, producing the wave-like behavior seen in Fig. 2. In Fig. 3a (pentad 32) the meridional peak in MSE and the

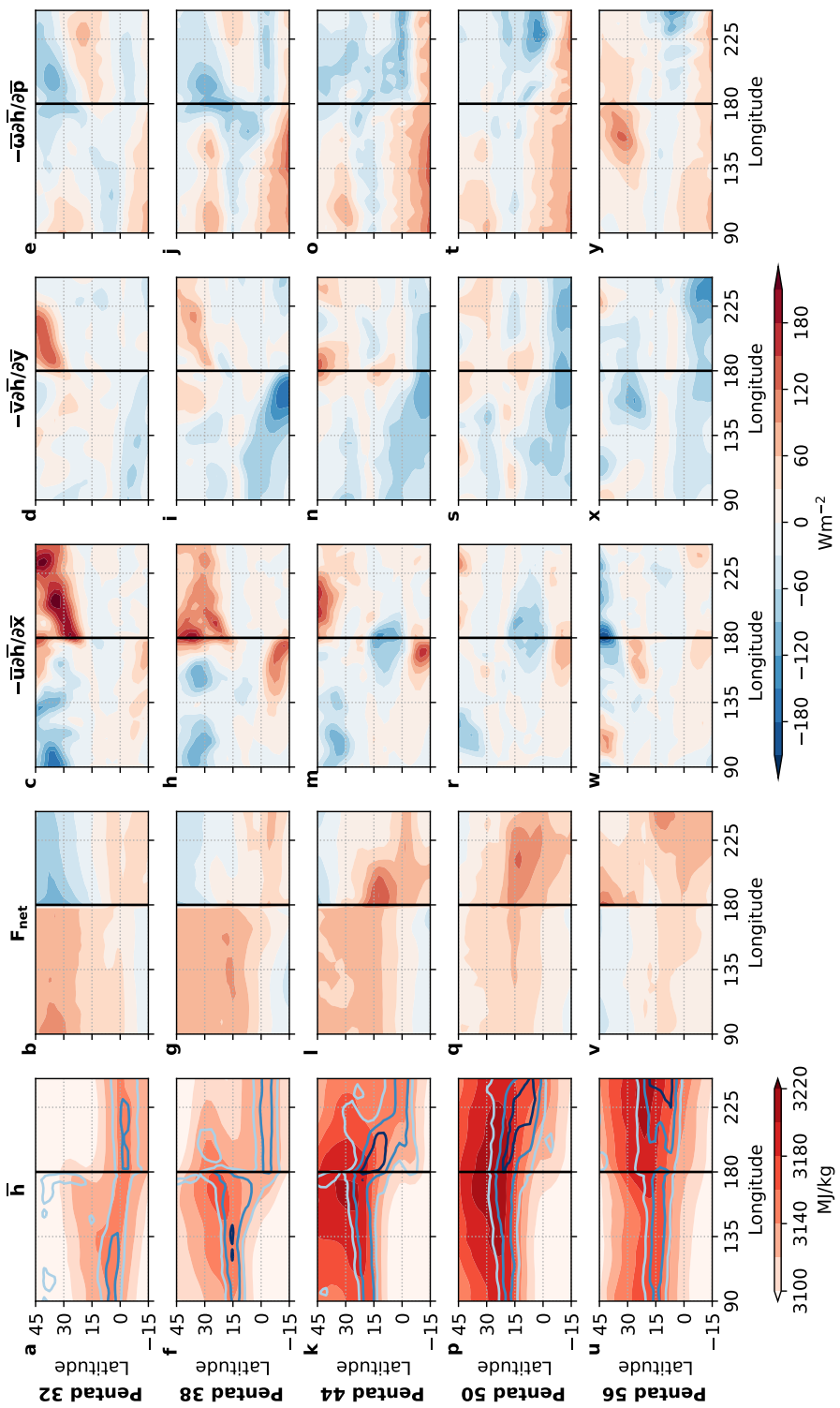

Figure 3. Maps of the column integrated MSE and the terms in the MSE budget (see Methods) for the half-land simulation. Black contours indicate the coastline. Blue contours in the lefthand column show precipitation, with interval 5mm/day. The terms and pentads shown are indicated by the column and row titles, respectively.

ITCZ are still near the Equator. The land has warmed in the Northern Hemisphere and a cross-equatorial circulation has begun to develop here, as indicated by the slight northward displacement of the ITCZ. Over land, the net energy fluxes into the column (F_{net}) act to increase the MSE of the column further (Fig. 3b), while near the Equator, the meridional circulation advects cooler, drier air up the MSE gradient, resulting in a net cooling (Figs. 3d&e). The result is a northward advance of the MSE peak and ITCZ by pentad 38 (Fig. 3f). These processes at work over the land are similar to those that have been identified in aquaplanet simulations (Bordoni & Schneider, 2008). However, in contrast with the aquaplanet, the cyclonic monsoon flow forced by the warm land generates southwesterly wind anomalies over the coastline at $\sim$ 20°N (Figs. 2a&d). These advect MSE down-gradient, warming and moistening the air columns over the ocean at $\sim$ 30°N, and extending the MSE maximum eastward (e.g. compare Figs. 3a,f&k). Accompanying this, the precipitation near the coastline migrates off the Equator, and the low-pressure anomaly and monsoon cyclone extend eastward. Once the monsoon westerlies extend over the ocean, these generate enhanced evaporation (Fig. 3l and see Fig. S2). This results in higher MSE over the ocean compared with the land. The westerlies are now advecting lower MSE air up-gradient, resulting in cooling over the coastline (Fig. 3m). As a result, in this simulation a MSE peak detaches from the coastline and migrates eastward through the remainder of the season.

Fig. 4 shows the MSE budget for the JRA-55 data, with CMAP precipitation overplotted in the lefthand column. Similar processes are seen to those identified in the idealized simulation: MSE increases over land and the MSE maximum then propagates eastward via downgradient MSE advection and evaporation of moisture by the monsoon westerlies (Fig. S3). However, some key differences are also evident. MSE increases first over the Indochina Peninsula and its westward spread is delayed. These effects appear to be predominantly generated by the interaction of the Tibetan Plateau with the circulation, with the MSE budget of the *simple-Asia* simulation, Fig. S4, showing similar behavior. At the beginning of the season (e.g. pentads 22-28) the Plateau generates southward flow on its Western side (Fig. 2c & f). This southward flow results in adiabatic descent, as indicated by the positive contribution of the $-\left\{\overline{\omega}\frac{\partial\overline{h}}{\partial p}\right\}$ term over India, Fig. 4e. This suggests that the earlier onset over the Bay of Bengal compared with India is not simply determined by enhanced moisture availability over the warm sea surface, but more by the delay of monsoon onset to the west due to the interaction of the westerly jet and the Tibetan Plateau.

The orography also influences the eastward propagation of the monsoon. In JRA-55, the Tibetan Plateau induces a stronger pressure anomaly than is forced in *half-land* (compare Figs 2a&b). In this simulation, the monsoon cyclone still expands eastward (rightmost column of Fig. 2), but travels more slowly and does not fully detach from the continent as seen in *half-land* for two reasons. First, the mechanical diversion of the wind around the orography forces a fixed low pressure centre which anchors the monsoon circulation. Second, the Indian ocean to the south retains heat for longer than the Southern Hemisphere land in the *half-land* simulation, so the MSE gradient reversal and advective cooling by the zonal flow seen in Figs. 3m&r do not occur (Figs. 4m&r and Figs S4m&r).

5 Discussion

Previous studies have considered the eastward progression of the monsoon as a passive response to delayed warming of the Western North Pacific SSTs (Wu & Wang, 2001; Wu, 2002; Hsu et al., 2014). Our simulations suggest a new perspective, that the monsoon circulation is a low-level planetary-scale cyclone, which expands northwestward and self-propagates eastward at a rate set by feedbacks from advection of MSE and wind-induced evaporation rather than by the solar forcing (see Fig. S1), whilst modifying the local Hadley and Walker circulations. Combined with interactions with the Tibetan Plateau,

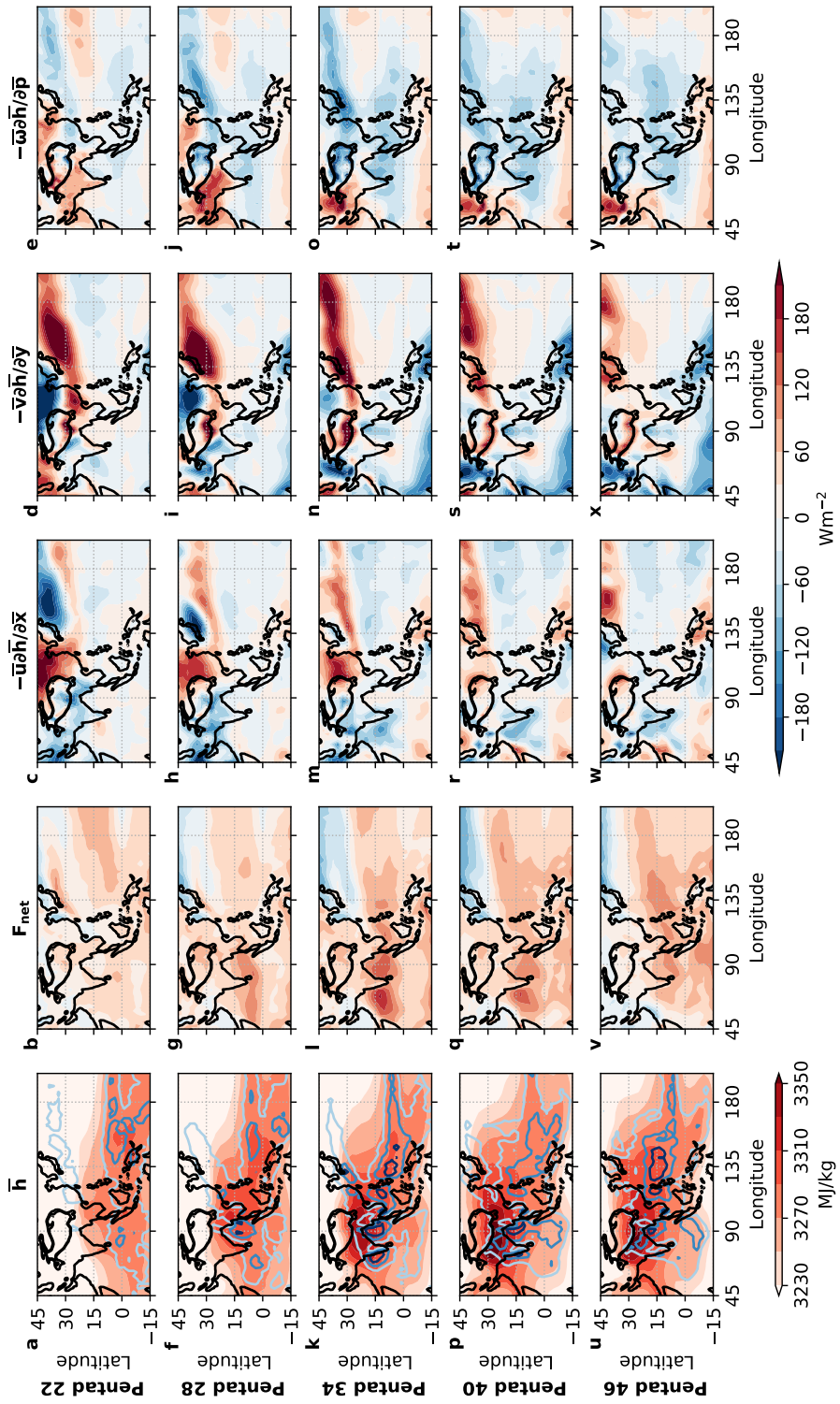

Figure 4. As 3, but based on JRA-55 data, with CMAP precipitation contours in the left-hand column. Black contours show the coastlines, and 2 and 3km orography contours.

these feedbacks result in the zoo of regional behaviors that are observed over Asia through the summer season. These results allow us to paint a new, unified view of the Asian monsoons, combining two seemingly opposing viewpoints. Monsoons were long considered as a large-scale sea breeze (Halley, 1686). In contrast, more recent theoretical work in aquaplanets has highlighted the role of land as a low thermal inertia surface in the monsoon, with land-sea contrast deemed non-essential for some basic monsoon-like behavior, such as the abrupt jumps in precipitation and changes in prevailing wind seen in the South Asian monsoon (Bordoni & Schneider, 2008). Our findings here bring the focus back onto land-sea contrast as an essential component of the large-scale Asian monsoon.

This convectively-coupled dynamical perspective provides a holistic explanation for the northwestward propagation of the monsoon rains over India (Bollasina & Ming, 2013; Parker et al., 2016) and the formation of the marine monsoon over the Western North Pacific (Wu & Wang, 2001). The understanding of the mechanisms governing the climatological Asian monsoon developed here provides a framework for explaining its patterns of variability and change: by altering the prevailing wind and temperature patterns, modes such as ENSO, or forcings from CO_2 and aerosols, will alter how the monsoon wave propagates throughout the season. In addition, we note that southwest-northeast bands of earlier onset are also seen around North America and over Africa, although more limited in extent (Fig. 2). Our *half-land* simulation is not specific to Asia, and it is likely that similar processes are important in other monsoon systems, providing a fundamental picture of a 'generic monsoon'. Last, of broader relevance, our results highlight a need to step beyond seasonal means when studying the large-scale circulation.

Acknowledgments

The work was supported by the UK-China Research and Innovation Partnership Fund, through the Met Office Climate Science for Service Partnership (CSSP) China, as part of the Newton Fund. GKV also acknowledges support from the Leverhulme Trust (RPG 2015-186) and NERC (NE/M006123). Datasets for this research are available in these in-text data citation references: Japan Meteorological Agency/Japan (2013); NOAA/OAR/ESRL (1995). Upon article acceptance, idealized model simulation data described in the study will be made available via the Open Research Exeter repository. For review purposes data has been uploaded to:

https://figshare.com/s/35cb0429d27661a27f3e

References

Betts, A. K. (1982). Saturation point analysis of moist convective overturning. *Journal of the Atmospheric Sciences*, *39*(7), 1484-1505. doi: 10.1175/1520-0469(1982)039⟨1484:SPAOMC⟩2.0.CO;2

Bollasina, M. A., & Ming, Y. (2013, Nov 01). The role of land-surface processes in modulating the indian monsoon annual cycle. *Climate Dynamics*, *41*(9), 2497–2509. Retrieved from `https://doi.org/10.1007/s00382-012-1634-3` doi: 10.1007/s00382-012-1634-3

Bordoni, S., & Schneider, T. (2008). Monsoons as eddy-mediated regime transitions of the tropical overturning circulation. *Nature Geoscience*, *1*(8), 515–519. doi: 10.1038/ngeo248

Bordoni, S., & Schneider, T. (2010). Regime Transitions of Steady and Time-Dependent Hadley Circulations: Comparison of Axisymmetric and Eddy-Permitting Simulations. *Journal of the Atmospheric Sciences*, *67*(5), 1643–1654. doi: 10.1175/2009JAS3294.1

Clough, S. A., Shephard, M. W., Mlawer, E. J., Delamere, J. S., Iacono, M. J., Cady-Pereira, K., ... Brown, P. D. (2005). Atmospheric radiative transfer modeling: A summary of the AER codes. *Journal of Quantitative Spectroscopy*

and Radiative Transfer, *91*(2), 233–244. doi: 10.1016/j.jqsrt.2004.05.058

Cui, K., & Shoemaker, S. P. (2018). A look at food security in China. *npj Sci Food*, *2*, 4. doi: 10.1038/s41538-018-0012-x

Emanuel, K. A. (1995). On Thermally Direct Circulations in Moist Atmospheres. *Journal of the Atmospheric Sciences*, *52*(9), 1529–1534. doi: 10.1175/1520-0469(1995)052⟨1529:OTDCIM⟩2.0.CO;2

Frierson, D. M. W., Held, I. M., & Zurita-Gotor, P. (2006). A Gray-Radiation Aquaplanet Moist GCM. Part I: Static Stability and Eddy Scale. *Journal of the Atmospheric Sciences*, *63*(10), 2548–2566. doi: 10.1175/JAS3753.1

Frierson, D. M. W., Lu, J., & Chen, G. (2007). Width of the Hadley cell in simple and comprehensive general circulation models. *Geophysical Research Letters*, *34*(18), 1–5. doi: 10.1029/2007GL031115

Gadgil, S., & Gadgil, S. (2006). The Indian monsoon, GDP and agriculture. *Econ. Polit. Weekly*, *41*, 4887-4895.

Geen, R., Bordoni, S., Battisti, D. S., & Hui, K. (2020). Monsoons, ITCZs and the Concept of the Global Monsoon. *Reviews of Geophysics*, *Accepted*.

Geen, R., Lambert, F. H., & Vallis, G. K. (2018). Regime Change Behavior During Asian Monsoon Onset. *Journal of Climate*, *31*, 3327–3348. Retrieved from `http://journals.ametsoc.org/doi/10.1175/JCLI-D-17-0118.1` doi: 10.1175/JCLI-D-17-0118.1

Geen, R., Lambert, F. H., & Vallis, G. K. (2019). Processes and Timescales in Onset and Withdrawal of 'Aquaplanet Monsoons'. *J. Atmos. Sci.*, *76*, 2357–2373. doi: 10.1175/JAS-D-18-0214.1

Gill, A. E. (1980). Some simple solutions for heat induced tropical circulation. *Quarterly Journal of the Royal Meteorological Society*, *106*(449), 447–462. doi: 10.1002/qj.49710644905

Halley, E. (1686). An Historical Account of the Trade Winds, and Monsoons, Observable in the Seas between and Near the Tropicks, with an Attempt to Assign the Phisical Cause of the Said Winds, By E. Halley. *Philosophical Transactions of the Royal Society of London*, *16*(179-191), 153–168. doi: 10.1098/rstl.1686.0026

Hsu, H.-H., Zhou, T., & Matsumoto, J. (2014). East Asian, Indochina and Western North Pacific Summer Monsoon - An Update. *Asia-Pacific J. Atmos. Sci.*, *50*(1), 45–68. doi: 10.1007/13143-014-0027-4

Huffman, G. J., Adler, R. F., Morrissey, M. M., Bolvin, D. T., Curtis, S., Joyce, R., ... Susskind, J. (2001). Global Precipitation at One-Degree Daily Resolution from Multisatellite Observations. *Journal of Hydrometeorology*, *2*, 36–50.

Japan Meteorological Agency/Japan. (2013). *JRA-55: Japanese 55-year Reanalysis, Daily, 3-Hourly and 6-Hourly Data.* Boulder CO: Research Data Archive at the National Center for Atmospheric Research, Computational and Information Systems Laboratory. Retrieved from `https://doi.org/10.5065/D6HH6H41`

Jucker, M., & Gerber, E. P. (2017). Untangling the annual cycle of the tropical tropopause layer with an idealized moist model. *Journal of Climate*, *30*(18), 7339-7358. doi: 10.1175/JCLI-D-17-0127.1

Kobayashi, S., Ota, Y., Harada, Y., Ebita, A., Moriya, M., Onoda, H., ... Takahashi, K. (2015). The jra-55 reanalysis: General specifications and basic characteristics. *J. Meteorol. Soc. Jpn.*, *93*(1), 5-48. doi: 10.2151/jmsj.2015-001

Lindberg, C., & Broccoli, A. J. (1996). Representation of topography in spectral climate models and its effect on simulated precipitation. *Journal of Climate*, *9*(11), 2641–2659. doi: 10.1175/1520-0442(1996)009⟨2641:ROTISC⟩2.0.CO;2

Matsuno, T. (1966). Quasi-Geostrophic Motions in the Equatorial Area. *J. Meteor. Soc. Japan*, *44*(1), 25–43. doi: 10.2151/jmsj1965.44.1_25

Mlawer, E. J., Taubman, S. J., Brown, P. D., Iacono, M. J., & Clough, S. A. (1997). Radiative transfer for inhomogeneous atmospheres: RRTM, a vali-

dated correlated-k model for the longwave. *Journal of Geophysical Research*, *102*(D14), 16 663–16 682. Retrieved from http://doi.wiley.com/10.1029/97JD00237 doi: 10.1029/97JD00237

Naylor, R. L., Battisti, D. S., Vimont, D. J., Falcon, W. P., & Burke, M. B. (2007). Assessing risks of climate variability and climate change for Indonesian rice agriculture. *Proceedings of the National Academy of Sciences*, *104*(19), 7752–7757. doi: 10.1073/pnas.0701825104

Nie, J., Boos, W. R., & Kuang, Z. (2010). Observational Evaluation of a Convective Quasi-Equilibrium View of Monsoons. *Journal of Climate*, *23*(16), 4416–4428. doi: 10.1175/2010JCLI3505.1

NOAA/OAR/ESRL. (1995). *CPC Merged Analysis of Precipitation (CMAP).* Boulder CO: Research Data Archive at the National Center for Atmospheric Research, Computational and Information Systems Laboratory. Retrieved from https://doi.org/10.5065/4QKP-PF57

O'Gorman, P. A., & Schneider, T. (2008). Energy of Midlatitude Transient Eddies in Idealized Simulations of Changed Climates. *Journal of Climate*, *21*(22), 5797–5806. doi: 10.1175/2008JCLI2099.1

Parker, D. J., Willetts, P., Birch, C., Turner, A. G., Marsham, J. H., Taylor, C. M., ... Martin, G. M. (2016). The interaction of moist convection and mid-level dry air in the advance of the onset of the Indian monsoon. *Quarterly Journal of the Royal Meteorological Society*, *142*(699), 2256-2272. Retrieved from https://rmets.onlinelibrary.wiley.com/doi/abs/10.1002/qj.2815 doi: 10.1002/qj.2815

Privé, N. C., & Plumb, R. A. (2007). Monsoon Dynamics with Interactive Forcing. Part I: Axisymmetric Studies. *Journal of the Atmospheric Sciences*, *64*(5), 1417–1430. doi: 10.1175/JAS3916.1

Rodwell, M. J., & Hoskins, B. J. (2001). Subtropical Anticyclones and Summer Monsoons. *Journal of Climate*, *14*(15), 3192–3211. doi: 10.1175/1520-0442(2001)014⟨3192:SAASM⟩2.0.CO;2

Saulière, J., Brayshaw, D. J., Hoskins, B., & Blackburn, M. (2012). Further Investigation of the Impact of Idealized Continents and SST Distributions on the Northern Hemisphere Storm Tracks. *Journal of the Atmospheric Sciences*, *69*(3), 840–856. Retrieved from http://centaur.reading.ac.uk/26373/{\%}5Cnhttp://journals.ametsoc.org/doi/abs/10.1175/JAS-D-11-0113.1 doi: 10.1175/JAS-D-11-0113.1

Schneider, T., & Bordoni, S. (2008). Eddy-Mediated Regime Transitions in the Seasonal Cycle of a Hadley Circulation and Implications for Monsoon Dynamics. *Journal of the Atmospheric Sciences*, *65*(1), 915–934. doi: 10.1175/2007JAS2415.1

Shaw, T. A. (2014). On the Role of Planetary-Scale Waves in the Abrupt Seasonal Transition of the Northern Hemisphere General Circulation. *Journal of the Atmospheric Sciences*, *71*(5), 1724–1746. doi: 10.1175/JAS-D-13-0137.1

Vallis, G., Colyer, G., Geen, R., Gerber, E., Jucker, M., Maher, P., ... Thomson, S. (2018). Isca, v1.0: A framework for the global modelling of the atmospheres of Earth and other planets at varying levels of complexity. *Geoscientific Model Development*, *11*, 843–859. doi: 10.5194/gmd-11-843-2018

Wang, B., & LinHo. (2002). Rainy Season of the Asian-Pacific Summer Monsoon. *Journal of Climate*, *15*, 386–398. doi: 10.1175/1520-0442(2002)015%3C0386:RSOTAP%3E2.0.CO;2

Wu, R. (2002). Processes for the northeastward advance of the summer monsoon over the Western North Pacific. *Journal of the Meteorological Society of Japan*, *80*(1), 67–83. doi: 10.2151/jmsj.80.67

Wu, R., & Wang, B. (2001). Multi-stage onset of the summer monsoon over the western North Pacific. *Climate Dynamics*, *17*(4), 277–289. doi: 10.1007/s003820000118

Xie, P., & Arkin, P. A. (1997). Global precipitation: A 17-year monthly analysis based on gauge observations, satellite estimates, and numerical model outputs. *Bulletin of the American Meteorological Society*, *78*(11), 2539-2558. Retrieved from `https://doi.org/10.1175/1520-0477(1997)078<2539:GPAYMA>2.0.CO;2` doi: 10.1175/1520-0477(1997)078⟨2539:GPAYMA⟩2.0.CO;2

Xie, S.-P., & Saiki, N. (1999). Abrupt Onset and Slow Seasonal Evolution of Summer Monsoon in an Idealized GCM Simulation. *J. Meteor. Soc. Japan*, *77*(4), 949–968. doi: 10.1248/cpb.37.3229

Yin, M. T. (1949). Synoptic-Aerologic Study of the Onset of the Summer Monsoon Over India and Burma. *Journal of Meteorology*, *6*(6), 393–400. doi: 10.1175/1520-0469(1949)006⟨0393:SASOTO⟩2.0.CO;2